Antiferromagnetic Heisenberg model on clusters with icosahedral symmetry

N. P. Konstantinidis*

Department of Physics and Department of Mathematics, University of Dublin, Trinity College, Dublin 2, Ireland
(Received 29 March 2005; published 31 August 2005)

The nearest-neighbor antiferromagnetic Heisenberg model is considered for spins $s_i = \frac{1}{2}$ and 1 located on the vertices of the dodecahedron and the icosahedron, which belong to the point symmetry group I_h. Taking into account the permutational and spin-inversion symmetries of the Hamiltonian results in a drastic reduction of the dimensionality of the problem, leading to full diagonalization for both clusters. There is a strong signature of the frustration present in the systems in the low-energy spectrum for $s_i = \frac{1}{2}$, where the first excited states are singlets. Frustration also results in a doubly peaked specific heat as a function of temperature for the dodecahedron. Furthermore, there is a discontinuity in the magnetization as a function of magnetic field for the dodecahedron, where a specific total spin sector never becomes the ground state in a field. This discontinuity is accompanied by a magnetization plateau. For $s_i = 1$ both systems again have singlet excitations. The magnetization of the dodecahedron has now two discontinuities in an external field and also magnetization plateaux, and the specific heat of the icosahedron, a two-peak structure as a function of temperature. The similarities between the two systems suggest that the antiferromagnetic Heisenberg model on a larger cluster with the same symmetry, the 60-site cluster, will have similar properties.

I. INTRODUCTION

The antiferromagnetic Heisenberg model has been the object of intense investigation in recent years as a prototype of strongly correlated electronic behavior.[1] The effects of low dimensionality, quantum fluctuations, and frustration combine together to produce phases different from conventional Néel-like order, where the order parameter is not the staggered magnetization or there is a lack of a local order parameter altogether.[2–4] They can also have dramatic consequences on the energy spectrum, as is the case for frustrated multiple spin-exchange models and the Kagomé lattice, where the low-energy excitations are singlets.[5] Specific-heat calculations of small Kagomé lattice samples have revealed a two-peak structure, with the first peak below the singlet-triplet gap.[6,7] The double-peak structure was also obtained for other multi-spin-exchange models,[8,9] a pyrochlore slab,[10] and the Δ chain.[11] It is a natural question to ask whether there are other frustrated systems with such unconventional behavior.

Here clusters with the connectivity of the fullerenes will be considered.[12,13] These molecules weakly bound to form crystals that become superconductors when doped with alkali metals.[14,15] Their transition temperature is above 40 K, a transition temperature much higher than the one of conventional superconductors. Chakravarty and Kivelson suggested that an electronic mechanism at intermediate scales is responsible for superconductivity in C_{60}, the fullerene with 60 carbon atoms, when doped with alkali metals.[16] It is an open question if a repulsive interaction can produce pairing in such systems. The Hubbard model has been used to investigate an electronic mechanism for superconductivity on this cluster.[17,18] Estimates for the nearest-neighbor hopping t and the on-site repulsion U are 2 to 3 eV and 9 eV respectively.[19,20] An exact treatment of the model in the full Hilbert space of the molecule is prohibitive because of its size. Therefore, as a first step, smaller molecules of the fullerene type were considered to gain insight, as well as the

strong on-site repulsion limit of the Hubbard model at half filling, the antiferromagnetic Heisenberg model, even though the 60-site molecule is in the intermediate U regime and not in the large U limit.[21,22] Coffey and Trugman found that connectivity and frustration lead to nontrivial behavior at the classical level in a magnetic field.[21] To study the effect of quantum fluctuations on the classical results, a 20-site cluster—the dodecahedron—was considered (Fig. 1). It is threefold coordinated, has all sites equivalent, and consists of 12 pentagons. The model was studied with perturbation theory for $s_i = \frac{1}{2}$ around the classical limit and was found to possess a singlet as the first excited state and a discontinuity in the magnetization as a function of quantum fluctuations.[23] This discontinuity was originally found at the classical level.[21] Therefore, it is of interest to study the structure of the low-energy spectrum of the dodecahedron and its response in a magnetic field for $s_i = \frac{1}{2}$. A more general question is if the presence of singlets in the excitation spectrum is also a property of other clusters, and if there is a correlation of magnetic behavior with space group symmetry and connectivity.[24] The
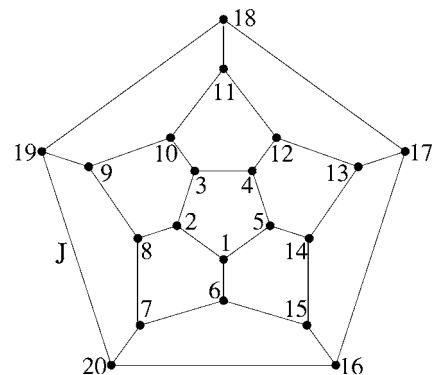

FIG. 1. Projection of the dodecahedron on a plane. The solid lines are antiferromagnetic bonds J. The black circles are spins s_i.
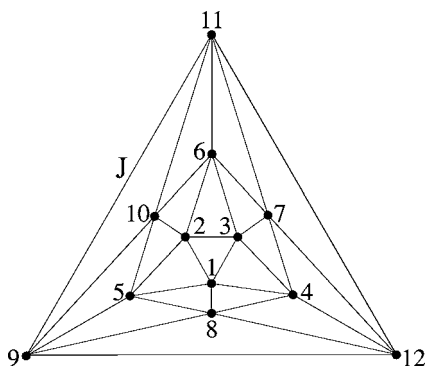
FIG. 2. Projection of the icosahedron on a plane. The solid lines are antiferromagnetic bonds J. The black circles are spins s_i.

determination of the full energy spectrum will reveal if the double-peak specific heat structure is also a property of the dodecahedron. However, the projection of the total spin on the z axis, S^z, is not a good quantum number when perturbing around the classical state. In addition, multiprecision arithmetic was needed to analytically continue the series expansions in Ref. 23. Thus, the full calculation of the energy spectrum was prohibited due to memory requirements, even though the symmetries of the Hamiltonian were partially taken into account. The ground-state properties of the model were calculated by Modine and Kaxiras.[25]

In this paper the antiferromagnetic Heisenberg model is studied on the dodecahedron and a smaller cluster with 12 equivalent sites and the same spatial symmetry, the icosahedron (Fig. 2), for $s_i = \frac{1}{2}$ and 1. The permutational and spin symmetries of the Hamiltonian are taken into account,[26–28] and this leads to full diagonalization except for the dodecahedron when $s_i = 1$, where Lanczos diagonalization is used.[29,30] The symmetry group of the clusters is I_h, the largest point symmetry group with 120 operations.[31] The icosahedron has 20 triangles, and the spins on the vertices are fivefold coordinated. Therefore, the two clusters share the same symmetry, but their connectivity is different. The results for the low-energy spectrum of the dodecahedron for $s_i = \frac{1}{2}$ show that the ground state is a singlet, whereas the first excited state is also a singlet, but fivefold degenerate. The next excited state is also a singlet, and then a series of states with total spin $S = 1$ follows. This series of low-lying singlets is a consequence of the connectivity and frustration of the model. The specific heat also shows a nonconventional behavior as a function of temperature, with a peak inside the energy gap and a second peak at higher temperatures. The low-energy spectrum of the icosahedron is similar to the one of the dodecahedron, with the same ordering and relative spacing of low energy levels. The specific heat has a well-pronounced peak inside the energy gap, but there is no second peak, rather a shoulder at higher temperatures. For spins with magnitude $s_i = 1$, the ground and first excited state of the dodecahedron are closely spaced singlets. The next excited state is a threefold degenerate triplet. The low-energy spectrum for the icosahedron is again the same in the symmetry, ordering, and relative spacing of the low-lying levels. The specific heat can only be calculated for the icosahedron and has now two peaks, however there is no peak inside the

energy gap. This along with the reduced number of low-energy singlet states compared to the full quantum $s_i = \frac{1}{2}$ case, indicates a change in the spectrum with increasing s_i.

The behavior of the magnetization in a magnetic field is nontrivial for the dodecahedron. There is a discontinuity as the energy of a particular S sector never becomes the ground state in a field. This feature, observed at the classical level by Coffey and Trugman,[21] survives in both the $s_i = \frac{1}{2}$ and 1 cases, twice in the latter. Similar behavior is not observed for the icosahedron, which also has discontinuous magnetization in a field at the classical level. Schröder *et al.* calculated the lowest quantum number with a discontinuity in a field to be $s_i = 4$.[32] However, for small fields and some of the lower s_i, the magnetization cannot be calculated due to memory requirements. Although the two clusters have the same spatial symmetry, the behavior in a field for small s_i appears to depend on their polygon structure. The magnetization discontinuities in the dodecahedron are accompanied by magnetization plateaux.

The similarities of the dodecahedron and icosahedron spectra suggest that predictions about the low-energy structure can be made for the larger cluster of fullerene-type connectivity with the same symmetry I_h, the 60-site cluster, where again all sites are equivalent.[13] Although the 12- and 20-site clusters have different coordination number and consist of different types of polygons, the structure of the low-energy spectrum is the same. The 60-site cluster has also a discontinuity in the magnetization in a field at the classical level.[21] However, it is not clear what the response in a magnetic field will be for the quantum case, since the two smaller clusters have different behavior for $s_i = \frac{1}{2}$ and 1, which seems to depend on the connectivity as well as their polygon structure. Similar considerations could correlate the behavior of more complicated models with orbital degrees of freedom, such as the Hubbard model on the 60-site cluster with the behavior of the same models on the dodecahedron and the icosahedron.

The plan of this paper is as follows: in Sec. II the model and method are introduced, in Sec. III the low-energy spectra of the two clusters are presented for both $s_i = \frac{1}{2}$ and 1, in Sec. IV specific heat and magnetic susceptibility data are presented, in Sec. V the ground-state magnetization is considered, and finally in Sec. VI the conclusions are presented.

II. MODEL AND METHOD

The Hamiltonian for the antiferromagnetic Heisenberg model is

$$H = J \sum_{\langle i,j \rangle} \vec{s}_i \cdot \vec{s}_j - h S^z, \tag{1}$$

where the spins $\vec{s}_i$ are located at the vertices of the clusters and $\langle i,j \rangle$ denotes nearest neighbors. The coupling constant J is positive and will be set to 1 from now on, defining the unit of energy. h is the strength of an external magnetic field.

Minimization of memory requirements for diagonalization is possible with the use of the symmetries of the model. These include permutational and spin-space symmetries.[26–28]

TABLE I. Low-energy spectrum for the icosahedron for $s_i=\frac{1}{2}$. The first index of the irreducible representations indicates the behavior under spatial inversion, where g stands for symmetric and u for antisymmetric,[31] and the second under spin inversion when $S^z=0$, where s stands for symmetric and a for antisymmetric.

Energy	Multiplicity	Irreducible representation	S	Energy	Multiplicity	Irreducible representation	S
−6.18789	1	$A_{u,s}$	0	−4.82887	5	$H_{u,s}$	0
−5.65445	5	$H_{g,s}$	0	−4.76398	5	$H_{u,a}$	1
−5.62426	1	$A_{g,s}$	0	−4.50000	4	$F_{g,s}$	0
−5.28801	3	$T_{2g,a}$	1	−4.50000	1	$A_{g,s}$	0
−5.17728	3	$T_{1u,a}$	1	−4.44972	4	$F_{u,a}$	1
−5.10989	3	$T_{2u,a}$	1	−4.31691	5	$H_{g,a}$	1
−4.86352	4	$F_{g,a}$	1	−4.29999	3	$T_{2u,a}$	1

The Hamiltonian commutes with S and S^z. However, even though it is straightforward to work in an S^z subspace, there is no efficient method to construct symmetry-adapted eigenstates of S. The Hamiltonian is symmetric under combinations of permutations of the spins that respect the connectivity of the cluster. The group of permutations is the symmetry group of the cluster in real space.[28] The model also posseses time-reversal symmetry, and inverting the spins is a symmetry operation in the $S^z=0$ sector. The corresponding group is comprised of the identity and the spin inversion operation. The full symmetry group of the Hamiltonian is the product of the space group and the group of spin inversion. Taking the full symmetry into account, the S^z basis states can be projected into states that transform under specific irreducible representations of the symmetry group. In this way the Hamiltonian is block diagonalized into smaller matrices, and their maximal dimension is dramatically reduced compared to the full Hilbert space size. The largest submatrix of the block-diagonalized Hamiltonian for the dodecahedron has dimension 7058 for spins $s_i=\frac{1}{2}$, and full diagonalization is possible. For $s_i=1$ only a few of the lowest eigenvalues for each irreducible representation were obtained with Lanczos diagonalization,[29,30] and for the subspace $S^z=1$ this was not possible for the five-dimensional representations. The largest matrix for which the lowest eigenvalue was found has dimensionality 13,611,598, and is complex. In the case of the icosahedron full diagonalization is possible for both $s_i=\frac{1}{2}$ and 1, the largest matrix having a dimension of 2982 in the latter case. It is noted that degeneracies are reported with respect to states with a specific value of S, and that each of these states has a number of $2S^z+1$ projections along the z-axis.

III. LOW-ENERGY SPECTRA AND CORRELATION FUNCTIONS

A. $s_i=\frac{1}{2}$

The low-energy spectrum of the icosahedron is presented in Table I. The ground state energy is a singlet and belongs to the irreducible representation $A_{u,s}$, where the first index g or u denotes symmetry or antisymmetry with respect to space

inversion,[31] and the second s or a symmetry or antisymmetry with respect to spin inversion when $S^z=0$. The energy per spin equals −0.51566. The first excited state is also a singlet, belongs to the representation $H_{g,s}$ and is fivefold degenerate. The next excited state is also an $S=0$ state, it is nondegenerate and belongs to $A_{g,s}$. Then a series of $S=1$ states follows. The gap to the first excited state is 0.5334 and the singlet-triplet gap 0.89988.

The nearest-neighbor correlation function for the ground state equals −0.20626, almost four times less in strength than the value of an isolated dimer, −0.75. For the first excited state there are two different types of nearest neighbor correlation functions. The first equals −0.16930 for the pairs (1,3), (9,11), (5,8), (6,7), (2,10), and (4,12) in Fig. 2, and the second −0.19328 for the rest of the bonds. The six pairs face each other in pairs and belong in different triangles. There are five different ways of distributing the pairs, thus the state is fivefold degenerate. The second excited singlet has all nearest-neighbor correlation functions equal to −0.18748. The correlation functions other than the nearest neighbor in the ground state between site 1 and the rest of the sites are equal to −0.13908 for spin 11, more than half the value of the nearest-neighbor correlation function, and 0.08408 for the rest of the spins.

The low-energy spectrum of the dodecahedron is shown in Table II and has the same structure as the one of the icosahedron, after comparison with Table I. In particular, the four lowest energy states belong to exactly the same irreducible representations as the corresponding states in the icosahedron. The spacing of the lowest energy states is also similar. The ground-state energy equals −9.72219,[23,25] and the energy per spin in the ground state is now higher and equal to −0.48611. Classically, the ground-state energy per bond is $-\sqrt{5}/3$ for the dodecahedron[23] and $-\sqrt{5}/5$ for the icosahedron (previously reported by Schmidt and Luban in Ref. 33); therefore, the energies per spin are equal. Quantum fluctuations reduce the energy more for the cluster with the highest coordination number, even though the number of bonds is the same for both. The gap to the first excited state is also smaller and equal to 0.31567, and the same is true for the singlet-triplet gap, which is 0.51383. The nearest-neighbor correlation function is equal to −0.32407 for the ground

TABLE II. Low-energy spectrum for the dodecahedron for $s_i=\frac{1}{2}$. Notation as in Table I.

Energy	Multiplicity	Irreducible representation	S	Energy	Multiplicity	Irreducible representation	S
−9.72219	1	$A_{u,s}$	0	−8.87964	5	$H_{u,s}$	0
−9.40651	5	$H_{g,s}$	0	−8.69499	3	$T_{2u,a}$	1
−9.35236	1	$A_{g,s}$	0	−8.69441	5	$H_{u,a}$	1
−9.20836	3	$T_{2g,a}$	1	−8.66571	3	$T_{1u,a}$	1
−9.18649	4	$F_{u,a}$	1	−8.65030	4	$F_{g,s}$	2
−9.13048	3	$T_{2u,a}$	1	−8.63614	5	$H_{g,a}$	1
−8.97112	3	$T_{1g,a}$	1	−8.63178	4	$F_{g,a}$	1

state,[23,25] quite stronger in magnitude than the one of the icosahedron, as in the classical case. This is attributed to the lower coordination number of the dodecahedron. For the first excited state, the value is −0.33585 for the pairs of spins numbered (1,2), (9,10), (14,15), (4,12), (17,18), (7,20) in Fig. 1; whereas for the rest of the pairs, it is −0.30797. The above six pairs are facing each other in pairs in the dodecahedron and belong in different pentagons. As in the icosahedron, there are five different ways of distributing the six pairs of spins in the above manner, thus the state is fivefold degenerate. The bonds on these pairs are more singletlike than the ground state, unlike the icosahedron. Another difference is that the bonds on the six pairs have now lower energy than the rest of the bonds. For the next excited state, the nearest-neighbor correlation functions are all equal to −0.31175. The correlation functions other than the nearest neighbor in the ground state between site 1 and the rest of the sites are equal to 0.06540 for spins 3, 4, 7, 8, 14, and 15; −0.03882 for spins 9, 10, 12, 13, 16, and 20; 0.03307 for spins 11, 17, and 19; and −0.03649 for spin 18. They are significantly smaller than the nearest-neighbor correlations. This is in contrast to the icosahedron, where correlations survive longer distances.

B. $s_i=1$

Full diagonalization is still possible for the icosahedron when $s_i=1$. The low-energy spectrum is shown in Table III. The ground state is a singlet in the $A_{g,s}$ irreducible representation, and its energy is −18.56111. It is now symmetric with respect to space inversion, in contrast to the $s_i=\frac{1}{2}$ case. The first excited state is a singlet in the $A_{u,s}$ representation, which

included the ground state for $s_i=\frac{1}{2}$, with energy close to the ground state and equal to −18.42539. The next excited state is a threefold degenerate triplet in the representation $T_{2u,a}$ with energy −17.83998, followed by another threefold degenerate triplet in the representation $T_{2g,a}$ with energy −17.80499. The energy per spin in the ground state is −1.54676 and the nearest-neighbor correlation function −0.61870. This value is to be compared to the singlet ground-state energy of a dimer with spins $s_i=1$, which equals −2. The ratio of the two values is larger compared to the corresponding ratio for the $s_i=\frac{1}{2}$ case and closer to the classical result. For the first excited state the nearest-neighbor correlation is −0.61418, much closer to the ground-state value compared to the $s_i=\frac{1}{2}$ case. The gap to the first excited state equals 0.13572 and the singlet-triplet gap 0.72113. The correlation functions other than the nearest neighbor in the ground state between site 1 and the rest of the sites are equal to −0.74630 for spin 11 and 0.36796 for the rest of the spins. Compared to the $s_i=\frac{1}{2}$ case, the magnitudes of the next-than-nearest-neighbor correlation functions are significantly increased with respect to nearest neighbors, and the correlation with site 11 is even stronger than the nearest-neighbor correlation.

As was the case for $s_i=\frac{1}{2}$, the low-energy spectrum (Table IV) is similar for the clusters when $s_i=1$. The ground state for the dodecahedron is a nondegenerate singlet with energy −30.24551 and an energy per spin equal to −1.51228. Again the energy per spin is higher than the one of the icosahedron. The first excited state is also a singlet close to the ground state with energy −30.21750, and the next two excited states are triply degenerate triplets with very close energies,

TABLE III. Low-energy spectrum for the icosahedron for $s_i=1$. Notation as in Table I.

Energy	Multiplicity	Irreducible representation	S	Energy	Multiplicity	Irreducible representation	S
−18.56111	1	$A_{g,s}$	0	−17.15212	3	$T_{1g,a}$	1
−18.42539	1	$A_{u,s}$	0	−17.00416	5	$H_{g,s}$	0
−17.83998	3	$T_{2u,a}$	1	−16.97485	4	$F_{u,a}$	1
−17.80499	3	$T_{2g,a}$	1	−16.82345	5	$H_{g,a}$	1
−17.60137	5	$H_{u,s}$	0	−16.75333	5	$H_{u,a}$	1
−17.19717	4	$F_{g,s}$	0	−16.74705	1	$A_{g,s}$	0
−17.17453	5	$H_{g,s}$	0	−16.73750	4	$F_{g,a}$	1

TABLE IV. Low-energy spectrum for the dodecahedron for $s_i=1$. Notation as in Table I. The S numbers in parentheses can be 0 or 1 since they are missing from the $S^z=2$ spectrum, and they are assigned values after comparison with the icosahedron low-energy spectrum in Table III.

Energy	Multiplicity	Irreducible representation	S	Energy	Multiplicity	Irreducible representation	S
−30.24551	1	$A_{g,s}$	0	−29.61145	3	$T_{1g,a}$	1
−30.21750	1	$A_{u,s}$	0	−29.57332	4	$F_{g,s}$	0
−29.92161	3	$T_{2u,a}$	1	−29.50512	3	$T_{1u,a}$	1
−29.91011	3	$T_{2g,a}$	1	−29.45063	4	$F_{g,a}$	1
−29.85881	5	$H_{g,s}$	(0)	−29.39457	5	$H_{u,a}$	(1)
−29.67223	5	$H_{u,s}$	(0)	−29.35464	5	$H_{g,a}$	(1)
−29.65951	4	$F_{u,a}$	1	−29.31754	3	$T_{2u,a}$	1

−29.92161 and −29.91011. The energy gap is 0.02801 and the singlet-triplet gap 0.32390, values again smaller than the ones of the icosahedron. The nearest-neighbor correlation functions in the ground and first excited states are equal to −1.00818 and −1.00725, respectively. The correlation functions other than the nearest neighbor in the ground state between site 1 and the rest of the sites are equal to 0.27896 for spins 3, 4, 7, 8, 14, and 15, −0.20912 for spins 9, 10, 12, 13, 16, and 20, 0.35962 for spins 11, 17, and 19, and −0.47333 for spin 18. Similarly to the icosahedron, the magnitudes are increased with respect to the nearest-neighbor correlations compared to the $s_i=\frac{1}{2}$ case. Farther-than-nearest-neighbor correlations are stronger for the icosahedron, as was the case for $s_i=\frac{1}{2}$. It was not possible to diagonalize the fivefold degenerate irreducible representations for $S^z=1$, and the S values in parentheses in Table IV are deduced by comparison to the similar low-energy spectrum of the icosahedron, since the spectra are similar. In any case, these S values can only be 0 or 1, with these energies absent from the $S^z=2$ spectrum.

IV. SPECIFIC HEAT AND MAGNETIC SUSCEPTIBILITY

The temperature dependence of the specific heat and the magnetic susceptibility for the cases where exact diagonalization is possible are shown in Figs. 3 and 4, respectively.
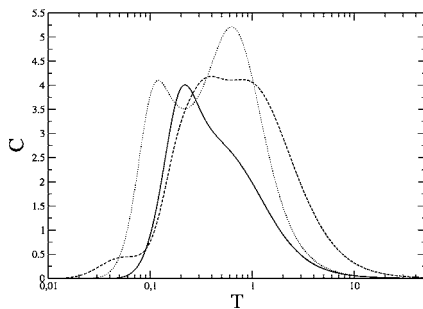
For the icosahedron and $s_i=\frac{1}{2}$, there is a peak in the specific heat around $T=0.219$ and a shoulder around $T=0.8$. The peak is inside the energy gap, a feature characteristic of frustrated systems.[6,7] For the dodecahedron there are two well-defined peaks. The first peak is centered around $T=0.120$ and the second around $T=0.627$. The first peak is inside the energy gap. Similar results have been obtained for other frustrated systems, and Sindzingre *et al.* attributed the peak to the combined effect of singlet excitations inside the singlet-triplet gap and low-lying triplet excitations for the Kagomé lattice.[6] In contrast, Syromyatnikov and Maleyev considered a Kagomé star where the peak results from the increase in the density of states just above the spin gap.[7] In the present case both the $S=0$ and $S=1$ sectors contribute for the peak inside the energy gap. The $S=0$ contribution is due to the low-lying singlets, whereas the $S=1$ contribution is also due to a few of the lowest energy triplets. For the shoulder and the higher energy peak in the two systems, respectively, higher S sectors contribute as well. For the icosahedron and $s_i=1$, there are three regions in the graph. At temperatures lower than the energy gap, the specific heat initially rises slowly toward an area between $T\approx0.055$ to 0.07, where it almost stabilizes with temperature. The contributions come from the lowest energy states in the $S=0$ and $S=1$ sectors. The specific heat then increases rapidly reaching a peak around $T=0.395$, followed by a slight decrease to a local minimum at a temperature around the singlet-triplet gap, T
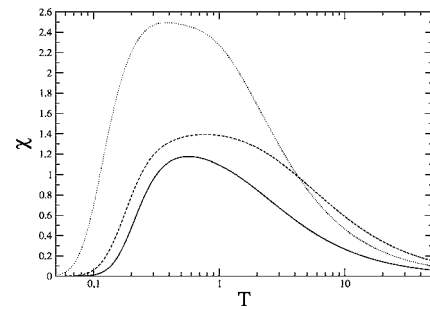

FIG. 3. Specific heat C of the nearest-neighbor antiferromagnetic Heisenberg model as a function of temperature T. Solid line: icosahedron with $s_i=\frac{1}{2}$, dotted line: dodecahedron with $s_i=\frac{1}{2}$, dashed line: icosahedron with $s_i=1$. C is in arbitrary units and T in units of energy.

FIG. 4. Magnetic susceptibility χ of the nearest-neighbor antiferromagnetic Heisenberg model as a function of temperature T. Solid line: icosahedron with $s_i=\frac{1}{2}$, dotted line: dodecahedron with $s_i=\frac{1}{2}$, dashed line: icosahedron with $s_i=1$. χ is in arbitrary units and T in units of energy.

TABLE V. Lowest energy in the various S sectors for the dodecahedron for $s_i=\frac{1}{2}$. Notation as in Table I.

S	Energy	Multiplicity	Irreducible Representation	S	Energy	Multiplicity	Irreducible Representation
0	−9.72219	1	$A_{u,s}$	6	−2.47099	1	$A_{u,s}$
1	−9.20836	3	$T_{2g,a}$	7	−0.13397	3	$T_{1u,a}$
2	−8.65030	4	$F_{g,s}$	8	2.34152	5	$H_{g,s}$
3	−7.72967	4	$F_{g,a}$	9	4.88197	3	$T_{2u,a}$
4	−6.40730	1	$A_{g,s}$	10	7.5	1	$A_{g,s}$
5	−4.37206	4	$F_{g,a}$				

=0.619. Following that it increases again to another peak around $T=0.786$ and then starts dropping toward zero. The contributions to the two peaks and the local minimum come from various spin sectors. Even though the double-peak structure is similar to the specific heat of the dodecahedron for $s_i=\frac{1}{2}$, there is no peak inside the energy gap, and this signifies a change with respect to the $s_i=\frac{1}{2}$ case. The magnetic susceptibility is plotted in Fig. 4, with a temperature dependence similar for the three cases. The position of the maximum follows the pattern for the lowest temperature peak of the specific heat, with a peak temperature decreasing with size and increasing with spin magnitude.

V. GROUND-STATE MAGNETIZATION

Frustrated spin systems have been found to exhibit magnetization jumps in the presence of an external field, where the lowest state in a particular S sector never becomes the ground state in the field.[34] The magnetization in an external field has been calculated for the dodecahedron at the classical level, and such a discontinuity was found.[21] A discontinuity in the magnetization was also found when the classical state is perturbed with the quantum fluctuations for $s_i=\frac{1}{2}$.[23] The calculation for the classical ground state of the icosahedron shows also the presence of a magnetization jump in a field. Taking the magnitude of the classical spins equal to 1, the saturation field for the dodecahedron is $h_s=3+\sqrt{5}$ and the discontinuity takes place at $h=0.26983\ h_s$. The magnetization jump is between $S^z=4.73765$ and 5.50362 (for the icosahedron the jump is between $S^z=4.71461$ and 5.10784, reported in Ref. 32). In the quantum case, the lowest energy in a magnetic field in a particular S sector is calculated from the lowest energy in the absence of a field by adding the Zeeman term. The lowest energies in the different S sectors are shown in Tables V and VI for the dodecahedron for $s_i=\frac{1}{2}$ and $s_i=1$, respectively. As was previously mentioned, calculation of the lowest energies is not possible for the five-dimensional irreducible representations when $S^z=1$. However, by comparing the spectra of the five-dimensional representations for $S^z=0$ with the spectra of the rest of the representations for $S^z=1$, it is seen that the lowest energy for $S=1$ does not belong to the five-dimensional representations (Table IV). The ground state magnetization is found by comparing the energies in a field in the different sectors. The plots for the dodecahedron for both $s_i=\frac{1}{2}$ and 1 are shown in Fig. 5, where the magnetization M is the total spin S normalized to the number of sites and the magnitude of each spin, with steps

TABLE VI. Lowest energy in the various S sectors for the dodecahedron for $s_i=1$. Notation as in Table I. For sectors with S higher than 1 the symmetry under spin inversion for the $S^z=0$ component has not been determined due to memory requirements (except for $S=20$).

| S	Energy	Multiplicity	Irreducible representation	S	Energy	Multiplicity	Irreducible representation
0	−30.24551	1	$A_{g,s}$	11	−9.72811	3	T_{2g}
1	−29.92161	3	$T_{2u,a}$	12	−6.26689	5	H_u
2	−29.30598	5	H_g	13	−2.61717	4	F_g
3	−28.39788	3	T_{1u}	14	1.22128	1	A_g
4	−27.20612	4	F_g	15	5.52324	3	T_{2g}
5	−25.49868	4	F_g	16	9.80295	1	A_u
6	−23.64370	1	A_g	17	14.65742	3	T_{1u}
7	−21.26717	4	F_g	18	19.65432	5	H_g
8	−18.82343	1	A_g	19	24.76393	3	T_{2u}
9	−15.88505	4	F_g	20	30	1	$A_{g,s}$
10	−12.98367	1	A_u				
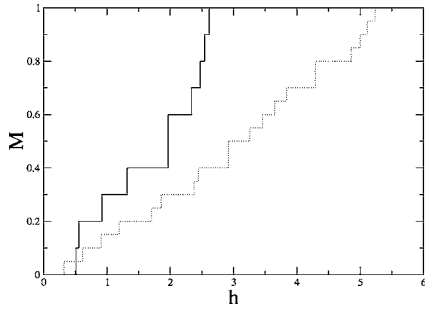
FIG. 5. Ground-state magnetization M as a function of magnetic field h for the dodecahedron. M is the total spin S normalized to the number of sites and the magnitude of spin. Solid line: $s_i=\frac{1}{2}$, dotted line: $s_i=1$. M has no units and h is in units of energy. The steps between S sectors are 0.1 for $s_i=\frac{1}{2}$ and 0.05 for $s_i=1$. The discontinuities are between 0.4 and 0.6 for $s_i=\frac{1}{2}$, and between 0.4 and 0.5, and 0.7 and 0.8 for $s_i=1$.

between different S sectors equal to 0.1 for $s_i=\frac{1}{2}$ and 0.05 for $s_i=1$. There is a discontinuity of M between 0.4 and 0.6 for $s_i=\frac{1}{2}$ ($S=4$ and 6), and two discontinuities for $s_i=1$, between 0.4 and 0.5 ($S=8$ and 10), and between 0.7 and 0.8 ($S=14$ and 16). These discontinuities are associated with magnetization plateaux on both sides of the jumps.[35] Magnetization plateaux are also observed in Fig. 5 for $M=0$ when $s_i=\frac{1}{2}$, and for $M=0.2$ and 0.3 for $s_i=1$. The saturation field is $h_{s1}=h_s/2$ for $s_i=\frac{1}{2}$, and the magnetization jump occurs at $h=0.75177\,h_{s1}$. For $s_i=1$, the saturation field is $h_{s2}=h_s$, and the jumps take place at $h=0.55765\,h_{s2}$ and $h=0.81948\,h_{s2}$.

As seen from Tables V and VI, the ground states on each side of the jumps are nondegenerate, and the spatial inversion symmetry of the ground state switches from symmetric to antisymmetric as the field increases. Spin-inversion symmetry has only be determined for $s_i=\frac{1}{2}$ for the cases of interest due to memory requirements, and in that case this symmetry does not change as the discontinuity takes place. The lowest state of M that never becomes the ground state is in every case symmetric with respect to spatial inversion, and it belongs to the same irreducible representation for the $s_i=\frac{1}{2}$ and the lowest field $s_i=1$ jump. It is also interesting that in the $s_i=1$ case, even though the lowest state for $S=6$ is nondegenerate (as is the $S=8$ state), there is no discontinuity associated with these two states, indicating the significance

of the different spatial inversion symmetry for the states on the two sides of a magnetization jump. However, a magnetization plateau exists for the corresponding magnetization $M=0.3$.

The behavior of the correlation functions on both sides of the magnetization jumps is shown in Table VII. The nearest-neighbor and next-nearest-neighbor correlation functions, as well as $\vec{S}_1\cdot\vec{S}_{11}$, become more positive as the magnetic field is getting stronger. For $\vec{S}_1\cdot\vec{S}_{18}$, the magnetization jump decreases its value with increasing field. However, this weakening is very pronounced for the $S=8$ to $S=10$ transition for $s_i=1$. For $\vec{S}_1\cdot\vec{S}_9$, the lower jump in the $s_i=1$ case decreases its strength, contrary to what happens for the other two discontinuities. It is concluded that the first discontinuity in the $s_i=1$ case has different characteristics from the other two jumps, as far as longer range correlation functions are concerned. This could possibly be due to different change in behavior with respect to spin inversion as this discontinuity takes place, compared to the other two discontinuities.

The data for the two lowest quantum numbers s_i shows that the discontinuity in the classical solution survives the quantum fluctuations. The presence of jumps for $s_i=\frac{1}{2}$, 1, and ∞ indicates that this is probably a characteristic of the system for any quantum number. The common features of the mechanism of the effect for the two lowest quantum numbers also point in this direction. For the icosahedron, there is no such jump for $s_i=\frac{1}{2}$ or 1, even though there is a jump at the classical level, and for $s_i=4$,[32] and quantum fluctuations are stronger. It is therefore concluded that the discontinuity in the magnetization at the full quantum level is not a consequence of the symmetry, but rather of the polygon structure of the clusters. For larger clusters with nonequivalent sites and including hexagons, no such discontinuity was found for $s_i=\frac{1}{2}$, even though there are jumps at the classical level.[24] Thus, the pentagon-only structure of the dodecahedron appears crucial for the presence of the discontinuities for the lowest s_i.

VI. CONCLUSIONS

The antiferromagnetic Heisenberg model was solved on the icosahedron and the dodecahedron, which belong to the point symmetry group I_h. It was found that the low-energy

TABLE VII. Ground-state correlation functions of spin 1 for the lowest energy states on both sides of the magnetization discontinuities for the dodecahedron. Correlations are the same between spin 1 and each of the spins in these groups: (2,5,6), (3,4,7,8,14,15), (9,10,12,13,16,20), (11,17,19), and (18) (see Fig. 1).

Correlation function	$s_i=\frac{1}{2}$ $S=4$	$s_i=\frac{1}{2}$ $S=6$	$s_i=1$ $S=8$	$s_i=1$ $S=10$	$s_i=1$ $S=14$	$s_i=1$ $S=16$
$\vec{S}_1\cdot\vec{S}_2$	−0.21358	−0.08237	−0.62745	−0.43279	0.04071	0.32677
$\vec{S}_1\cdot\vec{S}_3$	0.08764	0.12061	0.34296	0.43033	0.60512	0.72748
$\vec{S}_1\cdot\vec{S}_9$	0.04971	0.08038	0.18218	0.16926	0.47185	0.59169
$\vec{S}_1\cdot\vec{S}_{11}$	−0.01650	0.12180	−0.04887	0.36408	0.45061	0.73273
$\vec{S}_1\cdot\vec{S}_{18}$	0.11611	0.02574	0.47814	0.10860	0.56423	0.50655

spectra are similar and consist of excited states that are singlets for both $s_i = \frac{1}{2}$ and 1. Spin correlations survive longer distances for the icosahedron. The specific-heat calculation revealed a nontrivial dependence on temperature, with more than one peak for the dodecahedron for $s_i = \frac{1}{2}$, and the icosahedron for $s_i = 1$. This feature has also been found for other frustrated spin systems.[6–11] There are discontinuities in the ground-state magnetization as a function of magnetic field for the dodecahedron for both $s_i = \frac{1}{2}$ and 1, but this is not the case for the icosahedron. This discontinuity was found at the classical level,[21] and here it has been shown to survive the quantum fluctuations. It appears to be a characteristic of the system for any quantum number. There is also a number of magnetization plateaux for both quantum numbers. These nontrivial properties of the clusters are a consequence of the frustrated interactions and the connectivity. Other clusters of fullerene-type geometry show similar properties in their low-energy spectrum.[24] The similarities in the spectra and the specific heat of the icosahedron and the dodecahedron point in similar properties for the larger cluster with the same symmetry and 60 equivalent sites. It also shows that more complicated fermionic models for the 60-site system, such as the Hubbard model, could instead be considered on the icosahedron and the dodecahedron, and the results will be reliable predictions for the properties of the models on the larger system. However, no prediction can be made for the response in a field for the $s_i = \frac{1}{2}$ antiferromagnetic Heisenberg model, which depends not only on the symmetry, but also on the polygons that make up the clusters. At the classical level both the dodecahedron and the 60-site cluster have discontinuous magnetization in a field.[21] The dodecahedron exhibits jumps for both $s_i = \frac{1}{2}$ and 1 and has only pentagons, whereas the 60-site system has hexagons as well. It has been found that hexagon correlations are more important for frustrated systems of the fullerene type with more than 20 sites, for which there is no magnetization discontinuity for $s_i = \frac{1}{2}$, even though there are jumps at the classical level.[24] Another point deserving further attention is the transition from the quantum to the classical limit, regarding the low-energy spectra and the presence of singlets, the temperature dependence of the specific heat and the presence of magnetization discontinuities. The general behavior of the clusters with I_h point group symmetry is determined to a significant extent by the symmetry; however, the coordination number and the polygons that make up the structures are also important for the determination of their properties.

*Present address: Leoforos Syggroy 360, Kallithea 176 74, Athens, Hellas.

[1] E. Manousakis, Rev. Mod. Phys. **63**, 1 (1991).

[2] G. Misguich and C. Lhuillier, in *Frustrated Spin Systems*, edited by H. T. Diep (World Scientific, Singapore, 2003).

[3] C. Lhuillier and P. Sindzingre, in *Quantum Properties of Low-Dimensional Antiferromagnets*, edited by Y. Ajiro and J. P. Boucher (Kyushu University Press, Fukuoka, Japan, 2002).

[4] C. Lhuillier and G. Misguich, Proceedings of Summer School, *Trends in High Magnetic Field Science* (Springer Verlag, 2002), p.161–190; cond-mat/0109146.

[5] C. Waldtmann, H.-U. Everts, B. Bernu, C. Lhuillier, P. Sindzingre, P. Lecheminant, and L. Pierre, Eur. Phys. J. C **2**, 501 (1998).

[6] P. Sindzingre, G. Misguich, C. Lhuillier, B. Bernu, L. Pierre, C. Waldtmann, and H.-U. Everts, Phys. Rev. Lett. **84**, 2953 (2000).

[7] A. V. Syromyatnikov and S. V. Maleyev, J. Phys.: Condens. Matter **16**, S843 (2004).

[8] M. Roger, Phys. Rev. Lett. **64**, 297 (1990).

[9] G. Misguich, B. Bernu, C. Lhuillier, and C. Waldtmann, Phys. Rev. Lett. **81**, 1098 (1998).

[10] H. Kawamura and T. Arimori, Phys. Rev. Lett. **88**, 077202 (2002).

[11] K. Kubo, Phys. Rev. B **48**, 10552 (1993).

[12] H. W. Kroto, J. R. Heath, S. C. O'Brien, R. F. Curl, and R. E. Smalley, Nature (London) **318**, 162 (1985).

[13] P. W. Fowler and D. E. Manolopoulos, *An Atlas of Fullerenes* (Oxford University Press, London, 1995).

[14] A. F. Hebard, M. J. Roseeinsky, R. C. Haddon, D. W. Murphy, S. H. Glarum, T. T. M. Palstra, A. P. Ramirez, and A. R. Kortan, Nature (London) **350**, 600 (1991).

[15] K. Holczer, O. Klein, S.-M. Huang, R. B. Kaner, K.-J. Fu, R. L. Whetten, and F. Diederich, Science **252**, 1154 (1991).

[16] S. Chakravarty and S. A. Kivelson, Phys. Rev. B **64**, 064511 (2001).

[17] M. A. Ojeda, J. Dorantes-Dávila, and G. M. Pastor, Phys. Rev. B **60**, 9122 (1999).

[18] J. González and J. V. Alvarez, Phys. Rev. B **53**, 11729 (1996).

[19] S. Chakravarty, M. Gelfand, and S. Kivelson, Science **254**, 970 (1991).

[20] G. Stollhoff, Phys. Rev. B **44**, 10998 (1991).

[21] D. Coffey and S. A. Trugman, Phys. Rev. Lett. **69**, 176 (1992).

[22] D. Coffey and S. A. Trugman, Phys. Rev. B **46**, 12717 (1992).

[23] N. P. Konstantinidis and D. Coffey, Phys. Rev. B **63**, 184436 (2001).

[24] N. P. Konstantinidis, cond-mat/0503659.

[25] N. A. Modine and E. Kaxiras, Phys. Rev. B **53**, 2546 (1996).

[26] B. Bernu, P. Lecheminant, C. Lhuillier, and L. Pierre, Phys. Rev. B **50**, 10048 (1994).

[27] W. Florek and S. Bucikiewicz, Phys. Rev. B **66**, 024411 (2002).

[28] O. Waldmann, Phys. Rev. B **61**, 6138 (2000).

[29] R. Lehoucq, K. Maschhoff, D. Sorensen, and C. Yang, http://www.caam.rice.edu/software/ARPACK/.

[30] S. Shaw, http://www-heller.harvard.edu/shaw/programs/lapack.html.

[31] S. L. Altmann and P. Herzig, *Point-Group Theory Tables* (Oxford

University Press, London, 1994).

[32] C. Schröder, H.-J. Schmidt, J. Schnack, and M. Luban, Phys. Rev. Lett. **94**, 207203 (2005).

[33] H.-J. Schmidt and M. Luban, J. Phys. A **36**, 6351 (2003).

[34] J. Richter, J. Schulenburg, A. Honecker, J. Schnack, and H.-J. Schmidt, J. Phys.: Condens. Matter **16**, 779 (2004).

[35] A. Honecker, J. Schulenburg, and J. Richter, J. Phys.: Condens. Matter **16**, 749 (2004).